

---

# INTELLIGENT SYSTEM FOR AUTOMATED MOLECULAR PATENT INFRINGEMENT ASSESSMENT

---

Yaorui Shi<sup>1,2,\*</sup>, Sihang Li<sup>1,2,\*</sup>, Taiyan Zhang<sup>1</sup>, Xi Fang<sup>1</sup>, Jiankun Wang<sup>1</sup>,  
Zhiyuan Liu<sup>3</sup>, Guojiang Zhao<sup>1</sup>, Zhengdan Zhu<sup>1</sup>, Zhifeng Gao<sup>1</sup>, Renxin Zhong<sup>4</sup>,  
Linfeng Zhang<sup>1,5</sup>, Guolin Ke<sup>1</sup>, Weinan E<sup>2,5,6,7</sup>, Hengxing Cai<sup>1†</sup>, Xiang Wang<sup>2†</sup>

<sup>1</sup> DP Technology, Beijing, China

<sup>2</sup> University of Science and Technology of China, Hefei, Anhui, China

<sup>3</sup> National University of Singapore, Singapore

<sup>4</sup> School of Intelligent Systems Engineering, Sun Yat-Sen University, Shenzhen, China

<sup>5</sup> AI for Science Institute, Beijing, China

<sup>6</sup> School of Mathematical Sciences, Peking University, Beijing, China

<sup>7</sup> Center for Machine Learning Research, Peking University, Beijing, China

## ABSTRACT

Automated drug discovery offers significant potential for accelerating the development of novel therapeutics by substituting labor-intensive human workflows with machine-driven processes. However, a critical bottleneck persists in the inability of current automated frameworks to assess whether newly designed molecules infringe upon existing patents, posing significant legal and financial risks. We introduce PatentFinder, a novel tool-enhanced and multi-agent framework that accurately and comprehensively evaluates small molecules for patent infringement. It incorporates both heuristic and model-based tools tailored for decomposed subtasks, featuring: MarkushParser, which is capable of optical chemical structure recognition of molecular and Markush structures, and MarkushMatcher, which enhances large language models' ability to extract substituent groups from molecules accurately. On our benchmark dataset MolPatent-240, PatentFinder outperforms baseline approaches that rely solely on large language models, demonstrating a 13.8% increase in F1-score and a 12% rise in accuracy. Experimental results demonstrate that PatentFinder mitigates label bias to produce balanced predictions and autonomously generates detailed, interpretable patent infringement reports. This work not only addresses a pivotal challenge in automated drug discovery but also demonstrates the potential of decomposing complex scientific tasks into manageable subtasks for specialized, tool-augmented agents.

## 1 Introduction

Drug discovery [1, 2] remains a cornerstone in humanity's ongoing fight against disease, representing a vital pathway to improving global health outcomes. Traditional drug discovery [3] methods rely on wet-lab experiments and human expertise, rendering the process labor-intensive and time-consuming. To enhance efficiency and expedite the development of novel therapeutics, prior studies envision an automated drug discovery [4] pipeline, replacing manual workflows with machine-driven processes. This transition has shown remarkable potential in small-molecule drug discovery. Specifically, the advances in retrosynthesis planning [5–9], wet lab experiment automation [10–14], molecular docking [15–19], and de novo drug design [20–24] have demonstrated the feasibility of reducing human intervention while enhancing throughput and precision.

Despite these developments, AI models that learn existing drug data and structures to create new molecules may use protected compound structures during generation, leading to substantial legal and financial risks [25]. Such risk

---

\*Equal contribution.

†Correspondence authors: X.W. (xiangwang1223@gmail.com) and H.C. (caihengxing@dp.tech).

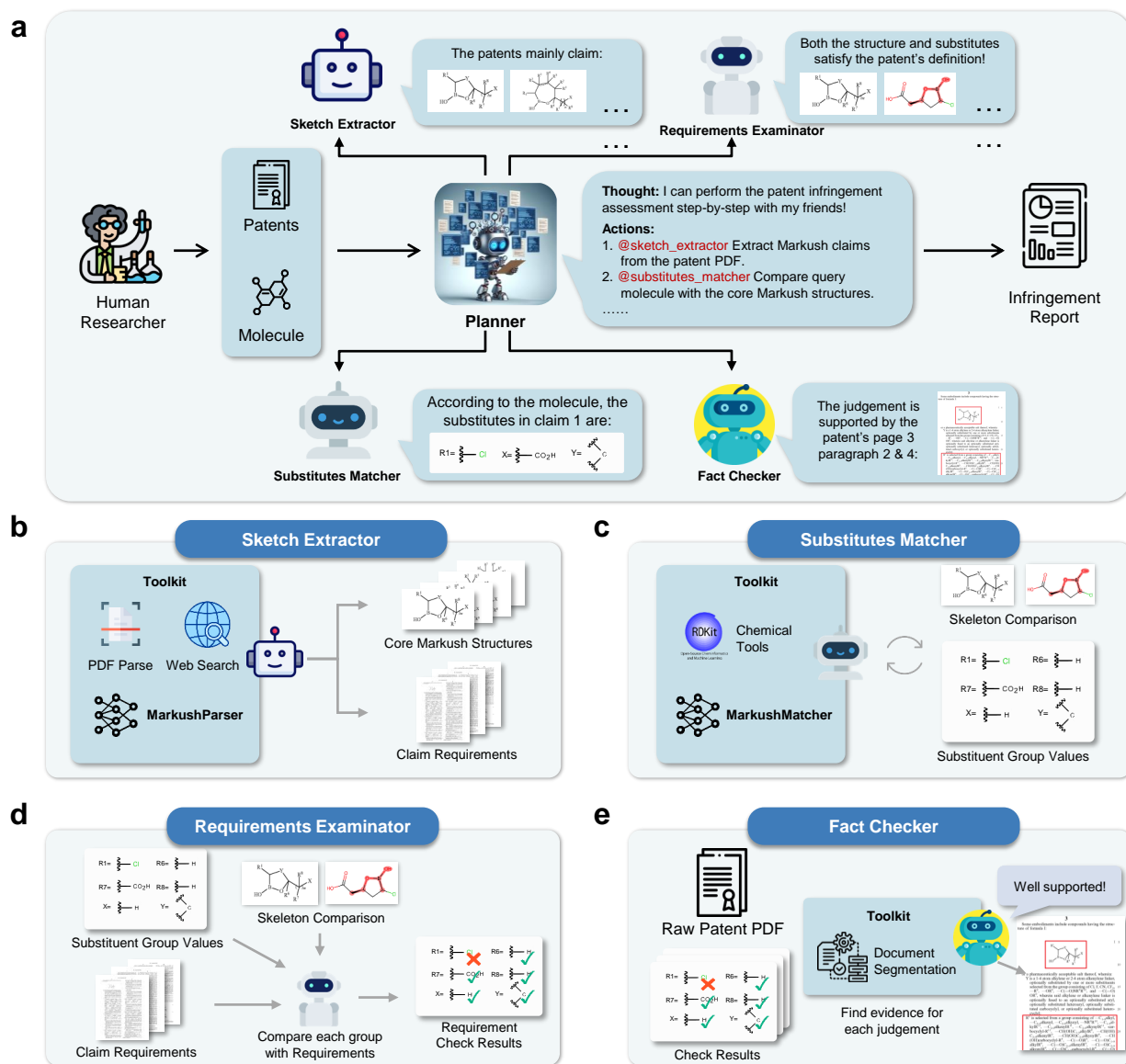


**Figure 1: Overview of PatentFinder.** a) Planner coordinates subtasks among agents and compiles a comprehensive infringement report. b) Skeleton Extractor extracts the core Markush structures and associated claim requirements from the Patent. c) Substitutes Matcher identifies and validates substituent groups in Markush expressions relative to the query molecule. d) Requirements Examiner assesses whether the query molecule meets the patent’s substituent group requirements. e) Fact Checker verifies agents’ outputs against original claims and corrects discrepancies for accuracy.

exists even for novel molecules, as they may still fall within the scope of existing patents due to overlapping Markush definitions or structural analogies. Current patentability assessments [26, 27] still heavily rely on manual inspection by pharmaceutical chemistry experts, which is labor-intensive, costly, and difficult to scale. This limitation hinders the realization of fully integrated, closed-loop automation, underscoring the need for an intelligent, end-to-end solution to streamline and enhance the patent assessment workflow.

Large language models (LLMs) [28–30] have demonstrated exceptional capabilities in analysis, reasoning, and problem-solving across diverse tasks [30–33]. Multimodal LLMs, in particular, extend these capabilities to interpret images [34–37] and PDF documents [38], making their potential applications in scientific domains, including drug discovery, increasingly practical. However, directly using LLMs for patent infringement assessment reveals several significant obstacles: (1) Inferior reasoning and lack of explainability. Without explicit stepwise guidance, LLMs often

generate hallucinations or biased judgments, with reasoning pathways that remain opaque. This lack of reliability and interpretability diminishes their suitability for high-stakes applications such as patent infringement assessment. (2) Limited capability in recognizing molecular structures. As shown in Fig.5, LLMs’ built-in image and PDF parsers struggle to interpret molecular and Markush diagrams in patent claims accurately. This deficiency hampers their ability to analyze essential structural details. (3) Inadequate recognition of substituent groups. Results in Fig.3 demonstrate that, when comparing candidate molecules to Markush definitions, LLMs frequently misinterpret molecular structures, resulting in incorrect predictions for substituent groups. (4) Absence of public patent infringement assessment benchmark. Although there are some open-source patent datasets available [39, 40], current researches lack a public benchmark for patent infringement assessment.

To overcome these challenges, we present PatentFinder, a novel end-to-end framework designed to accurately and comprehensively assess whether a molecule falls within the scope of a given patent. As illustrated in Fig.1, it adopts a tool-enhanced [41, 11, 42] and multi-agent [43–45] framework that decomposes the complex patent assessment task into manageable subtasks handled by specialized agents. The major innovations of PatentFinder include: (1) The multi-agent framework enables PatentFinder to generate intermediate outputs and compile them into a comprehensive infringement report, thereby enhancing the interpretability of the reasoning process. (2) We design a reverse data construction strategy and trained MarkushMatcher, which is capable of assisting LLMs in accurate substituent recognition; (3) MarkushParser, a Markush structure parsing tool model, which is trained to enable robust interpretation of molecular and Markush structures, even from complex visual representations; (4) To facilitate the evaluation of molecular patent infringement algorithms, we develop MolPatent-240, a molecular patent infringement evaluation benchmark that comprises 240 molecule-patent pairs.

Overall, extensive experiments in this paper demonstrate the following observations: (1) PatentFinder achieves state-of-the-art performance, significantly outperforming baseline approaches that rely solely on LLMs. Specifically, PatentFinder surpassed baselines by 13.8% in F1-score and 12% in accuracy, demonstrating its effectiveness in handling the nuanced demands of this task. (2) As illustrated in Fig.2e, PatentFinder autonomously generates comprehensive patent infringement reports. These reports integrate detailed molecular structure analyses and step-by-step reasoning, resulting in outputs that are both highly informative and easily interpretable. This capability represents a significant step forward in enhancing the transparency and usability of automated patent analysis solutions. Moreover, our approach of decomposing complex tasks into modular components, each managed by a specialized tool agent, holds potential for application in other scientific domains.

## 2 Results and Discussion

PatentFinder introduces two critical designs to facilitate the assessment of small-molecule patent infringement: (1) a multi-agent framework based on LLMs, where various agents equipped with tailored tools address relatively simple subtasks, and (2) two neural network models fine-tuned for specific tasks within the patent analysis process, addressing the performance deficiencies of LLMs in these tasks. To evaluate the effectiveness of these designs, we conduct separate experiments for each. For the assessment of PatentFinder’s multi-agent framework, we manually collect 70 real-world patents to construct the MolPatent-240 patent infringement benchmark and compare PatentFinder with state-of-the-art LLMs on small-molecule patent protection discrimination. For the fine-tuned tool models, we evaluate them on the tasks of Markush molecular structure matching and Markush image recognition. The experimental results demonstrate that these tool models effectively compensate for the deficiencies of general-purpose LLMs in Markush understanding tasks.

### 2.1 Evaluation of PatentFinder on MolPatent-240

#### 2.1.1 Experiment Settings

To demonstrate the effectiveness of PatentFinder for patent infringement assessment, we construct a patent protection benchmark – MolPatent-240. To illustrate the rationale behind our agent-based design, we compare PatentFinder with the direct prompting of leading LLMs, which are tasked with reasoning and determining whether a given molecule infringes on a patent without any additional guidance. The baselines include state-of-the-art large language models Gemini-1.5-Pro [38], Claude-3.5-Sonnet \*, GPT-4o [34], and OpenAI-o1 †. We leverage the Chain-of-Thought prompts [46] for all the baseline models to enhance their reasoning ability. As shown in Table 1, we explore three distinct schemes to assess these models for patent infringement assessment: (1) *Patent PDF*: In this scheme, the patent PDF file is directly provided to the LLM. This approach requires the model to have a built-in PDF parsing capability. (2)

\*[https://www-cdn.anthropic.com/de8ba9b01c9ab7cbabf5c33b80b7bbc618857627/Model\\_Card\\_Claude\\_3.pdf](https://www-cdn.anthropic.com/de8ba9b01c9ab7cbabf5c33b80b7bbc618857627/Model_Card_Claude_3.pdf).

†<https://openai.com/index/introducing-openai-o1-preview>

**Table 1:** Patent infringement assessment results on the MolPatent-240.

Method	F1-Score (↑)	Accuracy (↑)	Precision (↑)	TPR-TNR  (↓)	TPR(↑)	TNR(↑)
Random	50.0%	50.0%	43.3%	-	50.0%	50.0%
RDKit Algorithm	56.3%	59.0%	49.7%	41.6%	79.8%	38.2%
Tanimoto Similarity	57.1%	61.0%	50.3%	58.8%	90.4%	31.6%
<b># Patent PDF</b>						
Gemini-1.5-Pro	61.3%	56.1%	72.0%	77.5%	17.3%	<b>94.9%</b>
<b># Patent Text + Markush Image</b>						
GPT-4o	57.0%	61.5%	50.3%	69.3%	96.1%	26.9%
Claude-3.5-Sonnet	61.3%	65.7%	52.8%	66.7%	<b>99.0%</b>	32.4%
Gemini-1.5-Pro	65.8%	68.3%	57.0%	36.5%	86.5%	50.0%
<b># Patent Text + Markush String</b>						
GPT-4o	64.2%	65.2%	56.7%	15.7%	73.1%	57.4%
Claude-3.5-Sonnet	65.0%	68.6%	55.6%	53.3%	95.2%	41.9%
Gemini-1.5-Pro	70.8%	72.1%	62.5%	19.2%	81.7%	62.5%
OpenAI-o1	69.9%	71.2%	61.5%	18.8%	80.6%	61.8%
<b>PatentFinder</b>	<b>84.2%</b>	<b>84.1%</b>	<b>80.6%</b>	<b>0.9%</b>	83.7%	84.6%

*Patent Text + Markush Image:* The model is fed both the textual content of the patent and the core Markush structure images claimed in the patent. This scheme requires the model to handle both textual and visual information. (3) *Patent Text + Markush String:* In this case, all Markush images in the patent are first parsed into extended SMILES strings using our MarkushParser model. These Markush strings, along with the patent’s textual content, are then provided to LLMs in text format, allowing us to utilize text-only models in this scheme. Since the *Patent PDF* and *Patent Text + Markush Image* schemes require LLMs to handle PDF parsing and image processing, only Gemini, Claude, and GPT-4o are used for these experiments.

We also present the results of several heuristic methods. A structure matching algorithm based on RDKit performs skeleton matching between molecules and Markush structures in patents. If a molecule matches the skeleton of any Markush structure, it is considered to be protected by the patent. Based on the Tanimoto Similarity between the molecular structure and the patent’s Markush skeletons, molecules with a similarity greater than 0.5 are regarded as protected by the patent.

In our experiment, we utilize the following evaluation metrics: Micro F1-score, Balanced Accuracy, Precision, True Positive Rate (TPR), and True Negative Rate (TNR). Additionally, We calculate the absolute difference between TPR and TNR for each model to measure its predictive bias towards the True and False classes. We chose the F1 score as the primary metric for comparison. This metric balances precision and recall, ensuring equal emphasis on avoiding false positives and identifying true positives.

### 2.1.2 Results & Observations

Experimental results in Table 1 demonstrate that PatentFinder significantly outperforms the direct patent infringement classification with LLMs, regardless of the input scheme adopted. Specifically, our multi-agent collaboration framework achieves a 12.5% improvement in F1-score (relative to Gemini with patent text + Markush string) and an 11% increase in TNR (relative to Gemini with patent text + Markush image) compared to the best-performing baseline models.

These results highlight that instructing LLMs to perform patent assessment without stepwise guidance leads to severe hallucinations and suboptimal performance, which undermines both the reliability and interpretability of LLMs. In contrast, PatentFinder defines each tool-equipped agent clearly and decomposes the overall complex task into manageable subtasks. It then organizes multiple agents to address each subtask using the appropriate tools, resulting in a significant performance gain over baselines that use direct prompting methods.

We also observe that using Markush strings generated by MarkushParser instead of the raw Markush images within patents increases the accuracy of the baseline LLMs. As shown in the table, the patent text + Markush string approaches with Gemini, Claude, and GPT-4o show higher F1 scores (70.8%, 65.0%, and 64.2% respectively) compared to their patent text + Markush image versions (65.8%, 61.3%, and 57.0%). A similar result is observed when using the raw PDF input with Gemini (70.8% vs. 61.3%). These results suggest that VLMs struggle to interpret Markush structures through the vision modality. In contrast, our MarkushParser accurately converts Markush images into extended SMILES [47] representations using Optical Chemical Structure Recognition (OCSR), which is more digestible for LLMs whose training data consists predominantly of textual content.

Interestingly, we find that some popular LLMs (*e.g.*, GPT-4o and Claude-3.5-Sonnet) tend to adopt an overly conservative classification approach, frequently assuming that the query molecule is protected by the given patent. They exhibit a TPR that is significantly higher than their TNR, often by 50% or more. Notably, GPT-4o (patent text + Markush string) displays a TPR that exceeds its TNR by 69.2%. Given that MolPatent-240 has a roughly balanced positive-to-negative example ratio (1:1.3), this trend suggests that many leading LLMs tend to classify samples as positive indiscriminately, with some models performing worse than random guessing when distinguishing negative samples (TNR).

In contrast, PatentFinder demonstrates robust performance in distinguishing both positive and negative samples. It achieves a high TPR (83.7%) alongside a high TNR (84.6%), showcasing balanced and accurate classification across the MolPatent-240 dataset.

### 2.1.3 Case Studies

In real-world molecular patent infringement assessment, an effective and trustworthy collaboration between models and human experts requires the model to produce human-readable infringement analysis reports. These reports should not only deliver a definitive judgment on whether infringement has occurred but also provide a comprehensive and detailed explanation of intermediate reasoning steps. To this end, we evaluate not only the accuracy of the infringement assessment but also the validity of reasoning steps across different methods. Specifically, we compare the intermediate outputs of baseline models and PatentFinder on a real example from the MolPatent-240 dataset. The results are illustrated in Fig. 2. For baseline models, we summarize the step-by-step reasoning and final decisions of Gemini, GPT-4o, and Claude, while for PatentFinder, we present the intermediate outputs from each agent and the final infringement report generated by the Planner based on these analyses.

As shown in Fig. 2b, directly using LLMs for patent protection determination often leads to hallucinations in intermediate reasoning steps, resulting in incorrect conclusions based on non-existent evidence. For instance, Gemini provides no intermediate analysis and arrives at an incorrect judgment after merely comparing the molecular skeletons to the Markush structure. GPT-4o attempts to match the skeleton against the Markush structure but misidentifies the substituent D1 and introduces a fictitious substituent B. Although Claude reaches the correct conclusion, its analysis erroneously identifies R[21] as a chlorine atom and fails to determine the values of three other substituents.

From the baseline results, two key observations emerge: (1) Only GPT-4o attempts a fine-grained comparison of all substituents, while the other two methods deliver conclusions without detailed analysis. (2) LLMs exhibit limited capabilities in comparing chemical structures, with reasoning errors propagating through subsequent analysis steps.

PatentFinder addresses these challenges by employing a multi-agent framework that decomposes the complex task of patent infringement detection into a series of simpler subtasks. Each subtask is more comprehensible to a tool agent, enabling fine-grained analysis at every step. Additionally, the integration of domain-specific tools compensates for the shortcomings of pure LLM approaches in chemical structure analysis. This design significantly reduces the occurrence of hallucinations and reasoning errors. At the final stage, the Planner aggregates the outputs from all agents to generate a detailed infringement analysis report that includes a robust reasoning process.

## 2.2 Evaluation of MarkushMatcher

To showcase the ability of MarkushMatcher in delivering precise structural matching results, we curated a dataset comprising 1,000 samples for substituent extraction. The comparison focused on four key metrics: (1) **Accuracy**: The proportion of predictions that perfectly match the true substituent results. Perfect matches are defined as having a Tanimoto [48, 49] similarity of 100%. (2) **Validity**: The proportion of valid predictions. A prediction is considered valid if it includes all substituents mentioned in the Markush structure and each predicted substituent corresponds to a legitimate molecular structure. (3) **Average Tanimoto Similarity**: The average Tanimoto Similarity between each predicted substituent and its corresponding ground truth substituent, computed using Morgan Fingerprints [50] for all substituents in a sample, the higher the better. (4) **Levenshtein Distance**: The distance between the predicted results and the ground truth is calculated directly at the string level, the lower the better.

We compare MarkushMatcher with structure-matching baselines implemented using the rule-based – RDKit [51] and LLM-based – GPT-4o methods, respectively. As shown in Fig. 3a-c, MarkushMatcher outperforms both baseline methods on the substituent groups prediction task. As a deterministic algorithm, the rule-based approach – RDKit struggles with complex substituent matching tasks. While effective for simple tasks involving single-link substituents, it performs poorly in more intricate scenarios. This limitation resulted in near-zero accuracy and validity scores on our test set (*cf.* Fig. 3a,b), with unsatisfactory results for the other two metrics as well. Using LLMs alone does not yield satisfactory results either. Although GPT-4o is able to provide chemically valid solutions in many scenarios, which results in the high validity in Fig. 3c, it fails to predict the correct substituent group values in most cases, leading to low similarity, high Levenshtein distance, and limited accuracy. Common errors include: a) Confusing the values of

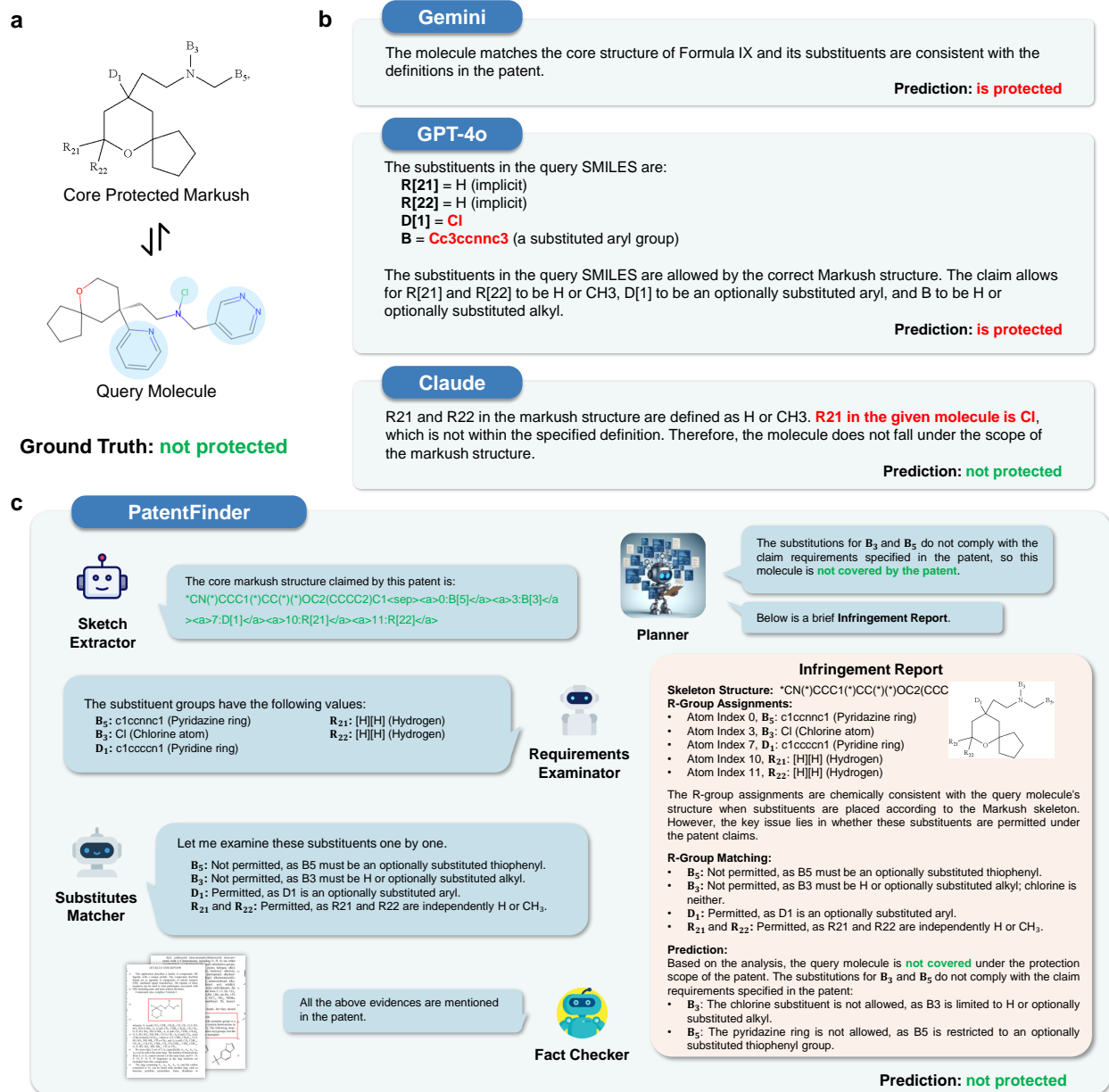


**Figure 2:** Case study on MolPatent-240. a) a random sample selected from MolPatent-240, the molecule is not protected by the patent. b, c, d) The prediction output of three baseline language models, both implemented with *Patent Text + Markush String* paradigm. e) The inference process of PatentFinder, in which different agents solve the subtasks separately, and their results are summarized into an infringement report.

different substituents; b) Incorrectly identifying substituent positions on the Markush structure; and c) Misclassifying scaffold atoms as part of the substituents. MarkushMatcher outperforms the other two methods by a large margin, with an accuracy of 66.8%. In comparison with GPT-4o, MarkushMatcher increases the mean average Tanimoto similarity from 21.3% to 92.9% and has an 8.8 times lower average Levenshtein distance. The training details of MarkushMatcher are presented in Fig. 3d, e. During the model's training, the training loss converges eventually, with a steady increase in both accuracy and validity. In the training data of MarkushMatcher, monatomic substituents such as C, N, and O are the most frequently occurring, while the heavy atom counts of other groups follow an approximately bell-shaped distribution.

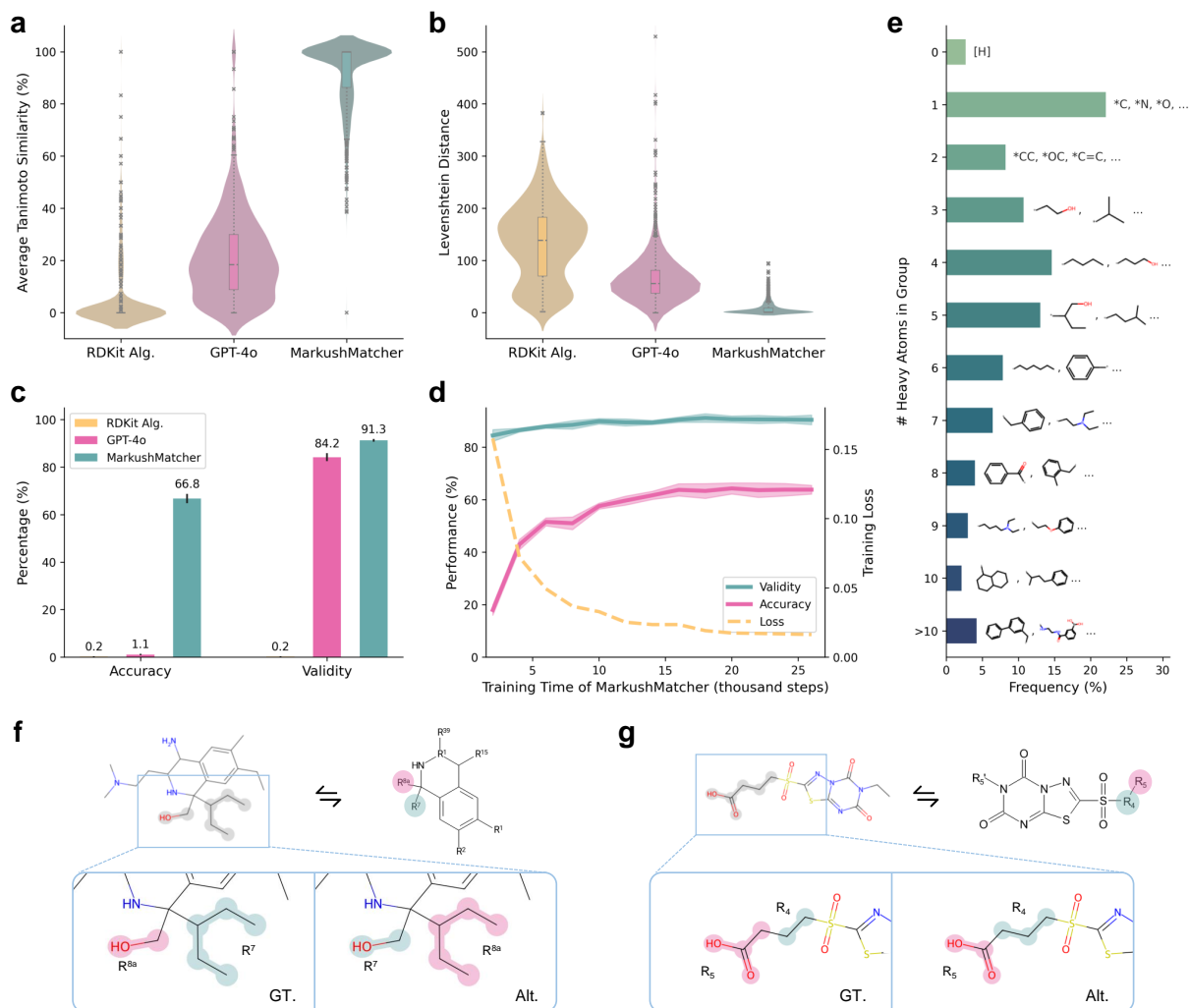


**Figure 3: Performance comparison between different substituent group extraction methods.** a) Average Tanimoto similarity of different matching algorithms. b) Levenshtein distances of different matching algorithms. c) Exact match accuracy and chemical validity of different matching algorithms. d) The accuracy, validity, and training loss of MarkushMatcher at different training steps. e) Statistics of the substituent groups used in training MarkushMatcher, where the groups with a single heavy atom (C, N, O) appear most frequently. f, g) The exchangeable groups and adjacent groups make the substituent group matching task unsolvable without additional textual description, which indicates the necessity of including contexts in the patent. GT: Ground Truth; Alt: Alternative solution.

We also find that in certain cases, even with the given Markush and molecular structures, it is impossible to determine a unique result without additional contextual information. For instance, the presence of exchangeable groups (*cf.* Fig.3f) and adjacent groups (*cf.* Fig.3g) in the Markush structures can introduce complexities. Specifically, if two substituent groups are connected to the same atom, the correlation between the group identifiers and the substructures may become ambiguous. Similarly, in cases where multiple substituent groups are adjacent, there could be various valid allocation schemes when specifying the group values.

In case these situations are commonly presented in the real-world patent Markush structures, we retain these data during the evaluation of substituent group extraction methodologies. Under these conditions, MarkushMatcher achieves a 92.9% Tanimoto Similarity, a remarkably high result considering the dataset’s complexity. Consequently, we employ the MarkushMatcher solely as a tool model within the PatentFinder pipeline, ensuring that the outputs of this model are meticulously validated by agents based on the complete content of the patent.

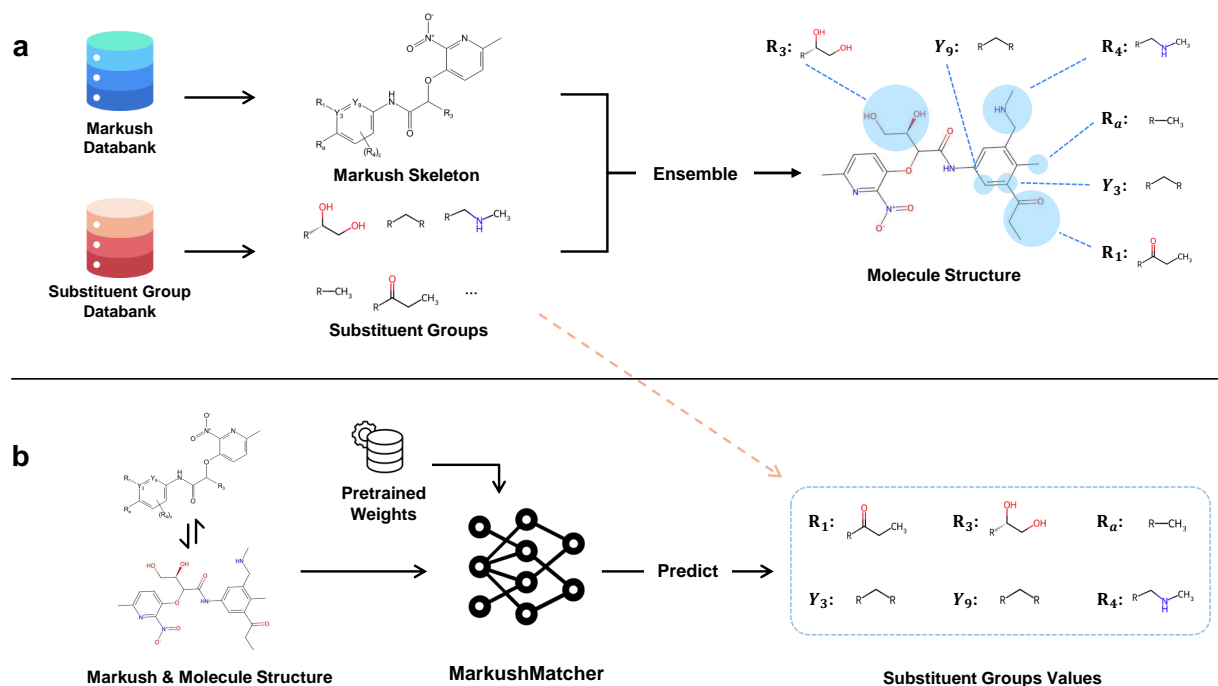


**Figure 4: Illustration of the development of MarkushMatcher.** a) The construction of Markush matching data, in which we design a reverse data generation algorithm by attaching the substituent groups onto the Markush Skeletons. b) During training, the MarkushMatcher model takes the Markush structure and the query molecule as input, and is trained to predict the values of each substituent group defined in the Markush structure.

### 2.3 Evaluation of MarkushParser

To demonstrate the effectiveness of MarkushParser in parsing Markush images into strings, we conduct experiments on MolPatent-240. We maintain the condition that the query molecules are always input in SMILES format and compared three different Markush input methods: original patent PDFs, Markush images, and Markush strings parsed by MarkushParser. We utilize three LLMs that support vision inputs – GPT-4o, Claude, and Gemini – to meticulously compare their intermediate outputs and the process of chain-of-thought reasoning under the different input modalities. The experimental results are shown in Table 1 and Fig.5a. The figure illustrates that the LLMs struggle to accurately understand the structure of Markush under the image and PDF understanding schemes, often erroneously fabricating Markush structures and non-existent substituent groups for analysis.

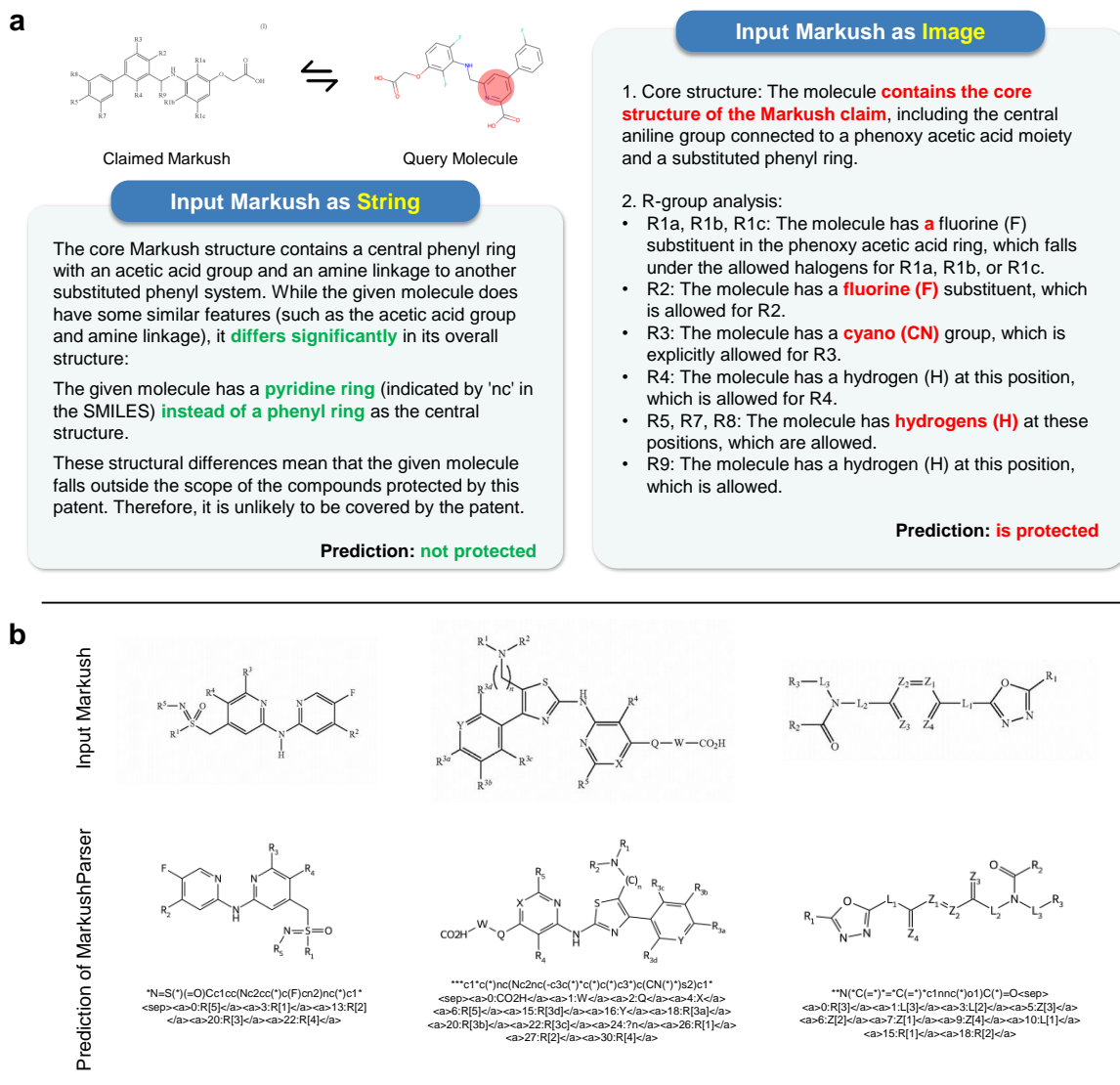
In Fig.5b, we present several results of the MarkushParser’s parsing of Markush images. The first row in the figure displays the original input Markush images, while the second row shows the extended SMILES strings generated by the MarkushParser and the reconstructed Markush structures based on these parsing results. The MarkushParser effectively captures the structural details of the Markush structures, and the reconstructed outputs exhibit high consistency with the original inputs.

## 3 Conclusion

PatentFinder drives automated drug discovery forward by tackling the critical challenge of patent infringement assessment for small molecular drugs. Through its novel tool-enhanced and multi-agent framework, PatentFinder addresses the inherent limitations of LLMs in interpreting complex molecular structures and Markush notations with precision and reliability.

Rigorous evaluations on the MolPatent-240 dataset highlight PatentFinder’s superior performance, achieving enhanced accuracy, balanced predictions, and improved interpretability. By autonomously generating detailed infringement reports, PatentFinder ensures transparency and usability in its assessments. It fills a crucial gap in the automated drug





discovery pipeline and enables seamless integration of patent compliance checks into pharmaceutical workflows, thus paving the way for more efficient and compliant pharmaceutical innovation.

## 4 Methods

### 4.1 Data Construction

This section outlines the data processing procedures applied to all datasets used in this paper.

#### 4.1.1 Construction of MolPatent-240

Due to the lack of publicly available molecular patent infringement datasets, we manually construct MolPatent-240 to facilitate evaluation. This dataset comprises 240 patent–molecule pairs, each labeled as either “protected” or “not protected” by human experts. To construct this dataset, we collect 70 molecular protection patents from public online sources, primarily including patents from WIPO (the World Intellectual Property Organization, prefixed with “WO”) and USPTO (the United States Patent and Trademark Office, prefixed with “US”). For positive examples, we select existing embodiments from the patents or manually designed novel molecules based on the patent claims. For negative examples, we modify the structures of positive examples at the atomic level, introducing subtle differences in the molecular skeleton or substituents that deviate from the patent claims. To ensure data accuracy, the dataset underwent multiple rounds of manual evaluation. After construction, three experts specializing in drug discovery verify the chemical correctness of all samples. This includes validating the legality of the constructed molecules and the correctness of their protection labels. Based on their feedback, individual dataset contributors revise the benchmark to correct errors and remove a subset of samples that are too challenging to rectify. The final dataset consists of 240 samples, including 104 positive examples (protected samples) and 136 negative examples (non-protected samples).

#### 4.1.2 Construction of Substituent Groups Extraction Data

Training MarkushMatcher requires large-scale data, which is impractical to annotate manually with human experts. Furthermore, the task of matching Markush structures with molecules and extracting substituent groups is exceptionally challenging, as rule-based algorithms and LLMs fail to produce satisfactory results. To address this, we propose a reverse data construction method that samples Markush structures and substituent groups from large-scale databases, assembles them into complete molecules using chemical tools, and records the substituent matching relationships during the assembly process. The entire pipeline is depicted in Fig.4.

MolParser-7M<sup>‡</sup>, a dataset containing over 7 million molecular and structural images, serves as the foundation for this process. Some samples in MolParser-7M include Markush structures. We heuristically design filtering rules to exclude unsuitable samples, such as those without Markush structures, those containing multiple molecules, or molecules that are excessively small. This filtering process results in a dataset of 847 thousand Markush structure records. We manually curate and organize a substituent group database containing 4.7k substituents derived from molecular structures. The distribution of the substituent groups in the training set is shown in Fig.3e. For each Markush sample in the dataset, we randomly sample substituent groups from this database according to the number of substituent attachment points on the scaffold. Using RDKit, we combine the Markush scaffold with the sampled substituents based on predefined rules to generate complete molecules. The substituent matching relationships are used as supervisory signals during the model’s training procedure.

Through this reverse construction method, we generate a dataset containing 847 thousand structural matching data. We randomly sample 1,000 examples from this dataset for model evaluation, with the results shown in Figure 3. The remaining samples are used to train MarkushMatcher.

#### 4.1.3 Construction of Markush OCSR Data

To facilitate the parsing of Markush diagrams in the patent, we collect 515 real-world Markush images, and manually label their corresponding string expressions. During labeling, we employ the extended SMILES notation defined in [47] to represent Markush structures as text. This dataset includes hand-drawn molecular images, Markush structures extracted from molecular protection patents, and other noisy samples.

The annotation process is conducted collaboratively by several researchers with expertise in medicinal chemistry, who meticulously label the Markush strings corresponding to each molecular image. This dataset serves as a valuable resource for finetuning MolParser to handle complex and noisy Markush recognition tasks.

<sup>‡</sup><https://huggingface.co/datasets/AI4Industry/MolParser-7M>

## 4.2 LLM-based Agents

We have designed multiple LLM-based agents to tackle subtasks, each fulfilling distinct roles:

**Planner.** As illustrated in Figure 1, this agent interacts directly with users by receiving input queries (i.e., patent and molecule) and providing output results (i.e., infringement report). The Planner collects the necessary information and determines which agent to engage next. Each time it decides to invoke an agent, it generates an instruction in the form of a triplet: (thought, target agent, input to agent). After sending the instruction to the target agent, the Planner awaits the “agent response” and continues to formulate new triplets based on the ongoing chat history. Once it determines that sufficient information has been gathered, it presents its infringement judgment to the user.

**Skeleton Extractor.** This agent is responsible for extracting the protected molecular skeletons from the patent. It supports reading patent content from both online sources and local PDF files with Patent Web Search and deployed parsing tool, respectively. It identifies key protected Markush structures and the associated claim requirements, specifically the substituent group values outlined in the patent.

**Substitutes Matcher.** This agent assesses the structural similarity between the query molecule and the extracted molecular skeleton to determine skeleton matches. It is equipped with a substructure matching algorithm and a substituent group extraction model. Both results from the matching algorithm and the extraction model are provided as references to this agent. Using vision-LLM (GPT-4o with image input), this agent verifies substituent group mappings, corrects chemical errors made during the substituent group extraction, and performs necessary rearrangements to the mappings based on the requirements.

**Requirements Examiner.** This agent compares the query molecule with the requirements defined in the patent, conducting the analysis at both the skeleton level and the substituent group level. At the skeleton level, the agent assesses the query molecule against the Markush structural skeleton and relevant requirements outlined in the patent (e.g., the overall number of heavy atoms or whether the molecule is explicitly discussed in the patent). For the substituent group level comparison, the agent evaluates the values of the substituent groups on the molecule against the definitions provided in the patent. After completing these comparisons, the agent reports the results to the Planner.

**Fact Checker.** This agent ensures that each requirement argument used in the previous reasoning steps is indeed present in the patent document. If the molecule is determined to be protected by the patent, the agent further identifies the core Markush structure that safeguards the molecule and locates the associated textual claim requirements. Subsequently, the agent utilizes the document segmentation model to divide the patent document and highlight the relevant claim requirement elements in the original PDF file for the user’s reference.

In our framework, we utilize two distinct LLMs: OpenAI-o1, which functions as the Requirement Examiner with a temperature setting of 1.0 to encourage reasoning, and GPT-4o, employed for other agents with a more conservative temperature setting of 0.2 to ensure consistent and accurate outputs.

### 4.2.1 Neural Network Tool Models

**MarkushMatcher.** The MarkushMatcher is a neural network model designed to predict the specific values of various substituents as defined by a given Markush structure in a queried molecule, based on the Markush structure and the molecular query.

MarkushMatcher is built upon the T5 [52], an encoder-decoder transformer [53] architecture, and is initialized with a MolT5-large [54] checkpoint. The training process of MarkushMatcher is illustrated in Figure 4b. To adapt the model for substituent group prediction, we fine-tune it using a large corpus of generated data. The input comprises molecular and Markush structures expressed as string representations, while the output, which maps substituent group values, is represented in JSON format. As detailed in Figure 4a, we construct a dataset of 847 thousand substituent group prediction samples for training and evaluation. The fine-tuning process involves training the model for one epoch on this dataset, using a batch size of 8 and a learning rate of  $1 \times 10^{-4}$ .

**MarkushParser.** MarkushParser converts molecular images into extended SMILES representations with OCSR (Optical Chemical Structure Recognition) and is capable of translating common molecules, substituent groups (incomplete molecules with connection points), and Markush structures.

This model uses Swin Transformer [55] as the image encoder and applies a two-layer multiple-layer perceptron as a vision-language connector similar to LLaVA [35]. After the vision encoder and connector, a BART model [56] decodes the compressed image features to predict the extended SMILES as text sequences.

We initialize MarkushParser with MolParser [47], which is pre-trained on a large annotated dataset consisting of 7.3 million samples, encompassing both real-world and synthetic image-SMILES pairs of molecules and Markush. We

manually collect and label 515 Markush images and their associated extended SMILES strings from real-world patent or drug discovery scenarios. We train the model using supervised fine-tuning (SFT) with our 515 Markush image-string pairs for 20 epochs with a learning rate of  $5 \times 10^{-5}$ .

**Document Segmentation.** The document segmentation tool, which is instantiated with a YOLO object detection model, recognizes all the elements in the PDF pages and locates their coordinates on the page. Each element could be a Markush/Molecular image, a table, or a paragraph in the PDF.

#### 4.2.2 Heuristic Tools

**Patent Web Search.** This function retrieves segmented molecular images and plain text content from the Google Patents database<sup>§</sup>. It is particularly useful for handling input queries when only the patent ID is provided. Notably, our framework remains fully functional without internet-based support, as it can alternatively rely on local PDF parsing and image processing through the OCSR scheme. This flexibility ensures that users can still perform comprehensive analyses even when web-based resources are unavailable.

**PDF Parser.** This tool converts the PDF patent document into images and texts, facilitating segmentation and extraction of key sections.

**RDKit Substructure Matcher.** We implement a substructure extraction algorithm with RDKit [51] to match the query molecule with the extracted Markush structure. Given the SMILES representation of a query molecule, this tool extracts the values of each substituent group defined in the Markush.

---

<sup>§</sup><https://patents.google.com/>

## References

- [1] Drews, J. Drug discovery: a historical perspective. *science* **287**(5460), 1960–1964 (2000).
- [2] Hughes, J. P., Rees, S., Kalindjian, S. B., and Philpott, K. L. Principles of early drug discovery. *British journal of pharmacology* **162**(6), 1239–1249 (2011).
- [3] Mandal, S., Mandal, S. K., et al. Rational drug design. *European journal of pharmacology* **625**(1-3), 90–100 (2009).
- [4] Schneider, G. Automating drug discovery. *Nature reviews drug discovery* **17**(2), 97–113 (2018).
- [5] Liu, B., Ramsundar, B., Kawthekar, P., Shi, J., Gomes, J., Luu Nguyen, Q., Ho, S., Sloane, J., Wender, P., and Pande, V. Retrosynthetic reaction prediction using neural sequence-to-sequence models. *ACS central science* **3**(10), 1103–1113 (2017).
- [6] Tetko, I. V., Karpov, P., Van Deursen, R., and Godin, G. State-of-the-art augmented nlp transformer models for direct and single-step retrosynthesis. *Nature communications* **11**(1), 5575 (2020).
- [7] Zhong, Z., Song, J., Feng, Z., Liu, T., Jia, L., Yao, S., Wu, M., Hou, T., and Song, M. Root-aligned smiles: a tight representation for chemical reaction prediction. *Chemical Science* **13**(31), 9023–9034 (2022).
- [8] Sacha, M., Błaz, M., Byrski, P., Dabrowski-Tumanski, P., Chrominski, M., Loska, R., Włodarczyk-Pruszyński, P., and Jastrzebski, S. Molecule edit graph attention network: modeling chemical reactions as sequences of graph edits. *Journal of Chemical Information and Modeling* **61**(7), 3273–3284 (2021).
- [9] Chen, S. and Jung, Y. Deep retrosynthetic reaction prediction using local reactivity and global attention. *JACS Au* **1**(10), 1612–1620 (2021).
- [10] Boiko, D. A., MacKnight, R., Kline, B., and Gomes, G. Autonomous chemical research with large language models. *Nat.* **624**(7992), 570–578 (2023).
- [11] Bran, A. M., Cox, S., Schilter, O., Baldassari, C., White, A. D., and Schwaller, P. Augmenting large language models with chemistry tools. *Nat. Mac. Intell.* **6**(5), 525–535 (2024).
- [12] Liu, Z., Shi, Y., Zhang, A., Li, S., Zhang, E., Wang, X., Kawaguchi, K., and Chua, T. Reactxt: Understanding molecular "reaction-ship" via reaction-contextualized molecule-text pretraining. In *Findings of the Association for Computational Linguistics, ACL 2024, Bangkok, Thailand and virtual meeting, August 11-16, 2024*, 5353–5377, (2024).
- [13] Vaucher, A. C., Schwaller, P., Geluykens, J., Nair, V. H., Iuliano, A., and Laino, T. Inferring experimental procedures from text-based representations of chemical reactions. *Nature communications* **12**(1), 2573 (2021).
- [14] Vaucher, A. C., Zipoli, F., Geluykens, J., Nair, V. H., Schwaller, P., and Laino, T. Automated extraction of chemical synthesis actions from experimental procedures. *Nature communications* **11**(1), 3601 (2020).
- [15] Abramson, J., Adler, J., Dunger, J., Evans, R., Green, T., Pritzel, A., Ronneberger, O., Willmore, L., Ballard, A. J., Bambrick, J., et al. Accurate structure prediction of biomolecular interactions with alphafold 3. *Nature* , 1–3 (2024).
- [16] Corso, G., Stärk, H., Jing, B., Barzilay, R., and Jaakkola, T. S. Diffdock: Diffusion steps, twists, and turns for molecular docking. In *The Eleventh International Conference on Learning Representations, ICLR 2023, Kigali, Rwanda, May 1-5, 2023*, (2023).
- [17] Zheng, S., Li, Y., Chen, S., Xu, J., and Yang, Y. Predicting drug–protein interaction using quasi-visual question answering system. *Nature Machine Intelligence* **2**(2), 134–140 (2020).
- [18] Tsaban, T., Varga, J. K., Avraham, O., Ben-Aharon, Z., Khramushin, A., and Schueler-Furman, O. Harnessing protein folding neural networks for peptide–protein docking. *Nature communications* **13**(1), 176 (2022).
- [19] Crampon, K., Giorkallos, A., Deldossi, M., Baud, S., and Steffanel, L. A. Machine-learning methods for ligand–protein molecular docking. *Drug discovery today* **27**(1), 151–164 (2022).
- [20] Sanchez-Lengeling, B. and Aspuru-Guzik, A. Inverse molecular design using machine learning: Generative models for matter engineering. *Science* **361**(6400), 360–365 (2018).
- [21] Bilodeau, C., Jin, W., Jaakkola, T., Barzilay, R., and Jensen, K. F. Generative models for molecular discovery: Recent advances and challenges. *Wiley Interdisciplinary Reviews: Computational Molecular Science* **12**(5), e1608 (2022).
- [22] Zhang, O., Zhang, J., Jin, J., Zhang, X., Hu, R., Shen, C., Cao, H., Du, H., Kang, Y., Deng, Y., et al. Resgen is a pocket-aware 3d molecular generation model based on parallel multiscale modelling. *Nature Machine Intelligence* **5**(9), 1020–1030 (2023).

- [23] Walters, W. P. and Barzilay, R. Applications of deep learning in molecule generation and molecular property prediction. *Accounts of chemical research* **54**(2), 263–270 (2020).
- [24] Li, S., Liu, Z., Luo, Y., Wang, X., He, X., Kawaguchi, K., Chua, T., and Tian, Q. Towards 3d molecule-text interpretation in language models. In *The Twelfth International Conference on Learning Representations, ICLR 2024, Vienna, Austria, May 7-11, 2024*, (2024).
- [25] Shimizu, Y., Ohta, M., Ishida, S., Terayama, K., Osawa, M., Honma, T., and Ikeda, K. Ai-driven molecular generation of not-patented pharmaceutical compounds using world open patent data. *J. Cheminformatics* **15**(1), 120 (2023).
- [26] Abraham, B. P. and Moitra, S. D. Innovation assessment through patent analysis. *Technovation* **21**(4), 245–252 (2001).
- [27] Lemley, M. A. Inducing patent infringement. *UC Davis L. Rev.* **39**, 225 (2005).
- [28] Devlin, J., Chang, M., Lee, K., and Toutanova, K. BERT: pre-training of deep bidirectional transformers for language understanding. In *Proceedings of the 2019 Conference of the North American Chapter of the Association for Computational Linguistics: Human Language Technologies, NAACL-HLT 2019, Minneapolis, MN, USA, June 2-7, 2019, Volume 1 (Long and Short Papers)*, 4171–4186, (2019).
- [29] Bommasani, R. and et al. On the opportunities and risks of foundation models. (2021). Preprint at <https://arXiv.org/abs/2108.07258>.
- [30] Brown, T. B., Mann, B., Ryder, N., Subbiah, M., et al. Language models are few-shot learners. In *Advances in Neural Information Processing Systems 33: Annual Conference on Neural Information Processing Systems 2020, NeurIPS 2020, December 6-12, 2020, virtual*, (2020).
- [31] Ouyang, L., Wu, J., Jiang, X., Almeida, D., Wainwright, C., Mishkin, P., Zhang, C., Agarwal, S., Slama, K., Ray, A., et al. Training language models to follow instructions with human feedback. *Advances in neural information processing systems* **35**, 27730–27744 (2022).
- [32] Taylor, R., Kardas, M., Cucurull, G., Scialom, T., Hartshorn, A., Saravia, E., Poulton, A., Kerkez, V., and Stojnic, R. Galactica: A large language model for science. (2022). Preprint at <https://arXiv.org/abs/2211.09085>.
- [33] Touvron, H., Lavril, T., Izacard, G., Martinet, X., Lachaux, M., Lacroix, T., Rozière, B., Goyal, N., Hambro, E., Azhar, F., Rodriguez, A., Joulin, A., Grave, E., and Lample, G. Llama: Open and efficient foundation language models. (2023). Preprint at <https://arXiv.org/abs/2302.13971>.
- [34] OpenAI. Gpt-4o system card. (2024). Preprint at <https://arXiv.org/abs/2410.21276>.
- [35] Liu, H., Li, C., Wu, Q., and Lee, Y. J. Visual instruction tuning. In *Advances in Neural Information Processing Systems 36: Annual Conference on Neural Information Processing Systems 2023, NeurIPS 2023, New Orleans, LA, USA, December 10 - 16, 2023*, (2023).
- [36] Wu, S., Fei, H., Qu, L., Ji, W., and Chua, T. Next-gpt: Any-to-any multimodal LLM. In *Forty-first International Conference on Machine Learning, ICML 2024, Vienna, Austria, July 21-27, 2024*, (2024).
- [37] OpenAI. GPT-4 technical report. (2023). Preprint at <https://arXiv.org/abs/2303.08774>.
- [38] Google, G. T. Gemini: A family of highly capable multimodal models. (2023). Preprint at <https://arXiv.org/abs/2312.11805>.
- [39] Papadatos, G., Davies, M., Dedman, N., Chambers, J., Gaulton, A., Siddle, J., Koks, R., Irvine, S. A., Pettersson, J., Goncharoff, N. T., Hersey, A., and Overington, J. P. Surechembl: a large-scale, chemically annotated patent document database. *Nucleic Acids Res.* **44**(Database-Issue), 1220–1228 (2016).
- [40] Morin, L., Weber, V., Meijer, G. I., Yu, F., and Staar, P. W. Patcid: an open-access dataset of chemical structures in patent documents. *Nature Communications* **15**(1), 6532 (2024).
- [41] Schick, T., Dwivedi-Yu, J., Dessì, R., Raileanu, R., Lomeli, M., Hambro, E., Zettlemoyer, L., Cancedda, N., and Scialom, T. Toolformer: Language models can teach themselves to use tools. *Advances in Neural Information Processing Systems* **36** (2024).
- [42] Kang, Y. and Kim, J. Chatmof: an artificial intelligence system for predicting and generating metal-organic frameworks using large language models. *Nature Communications* **15**(1), 4705 (2024).
- [43] Dorri, A., Kanhere, S. S., and Jurdak, R. Multi-agent systems: A survey. *Ieee Access* **6**, 28573–28593 (2018).
- [44] Zhang, A., Chen, Y., Sheng, L., Wang, X., and Chua, T. On generative agents in recommendation. In *Proceedings of the 47th International ACM SIGIR Conference on Research and Development in Information Retrieval, SIGIR 2024, Washington DC, USA, July 14-18, 2024*, 1807–1817, (2024).

- [45] Qian, C., Liu, W., Liu, H., Chen, N., Dang, Y., Li, J., Yang, C., Chen, W., Su, Y., Cong, X., Xu, J., Li, D., Liu, Z., and Sun, M. Chatdev: Communicative agents for software development. In *Proceedings of the 62nd Annual Meeting of the Association for Computational Linguistics (Volume 1: Long Papers), ACL 2024, Bangkok, Thailand, August 11-16, 2024*, 15174–15186, (2024).
- [46] Wei, J., Wang, X., Schuurmans, D., Bosma, M., Ichter, B., Xia, F., Chi, E. H., Le, Q. V., and Zhou, D. Chain-of-thought prompting elicits reasoning in large language models. In *Advances in Neural Information Processing Systems 35: Annual Conference on Neural Information Processing Systems 2022, NeurIPS 2022, New Orleans, LA, USA, November 28 - December 9, 2022*, (2022).
- [47] Fang, X., Wang, J., Cai, X., Chen, S., Yang, S., Yao, L., Zhang, L., and Ke, G. Molparser: End-to-end visual recognition of molecule structures in the wild. (2024). Preprint at <https://arxiv.org/abs/2411.11098>.
- [48] Bajusz, D., Rácz, A., and Héberger, K. Why is tanimoto index an appropriate choice for fingerprint-based similarity calculations? *J. Cheminformatics* **7**, 20:1–20:13 (2015).
- [49] Tanimoto, T. T. Elementary mathematical theory of classification and prediction. *International Business Machines Corporation* (1958).
- [50] Morgan, H. L. The generation of a unique machine description for chemical structures—a technique developed at chemical abstracts service. *Journal of chemical documentation* **5**(2), 107–113 (1965).
- [51] Landrum, G. Rdkit documentation. *Release* **1**(1-79), 4 (2013).
- [52] Raffel, C., Shazeer, N., Roberts, A., Lee, K., Narang, S., Matena, M., Zhou, Y., Li, W., and Liu, P. J. Exploring the limits of transfer learning with a unified text-to-text transformer. *J. Mach. Learn. Res.* **21**, 140:1–140:67 (2020).
- [53] Vaswani, A., Shazeer, N., Parmar, N., Uszkoreit, J., Jones, L., Gomez, A. N., Kaiser, L., and Polosukhin, I. Attention is all you need. In *Advances in Neural Information Processing Systems 30: Annual Conference on Neural Information Processing Systems 2017, December 4-9, 2017, Long Beach, CA, USA*, 5998–6008, (2017).
- [54] Edwards, C., Lai, T. M., Ros, K., Honke, G., Cho, K., and Ji, H. Translation between molecules and natural language. In *Proceedings of the 2022 Conference on Empirical Methods in Natural Language Processing, EMNLP 2022, Abu Dhabi, United Arab Emirates, December 7-11, 2022*, 375–413, (2022).
- [55] Liu, Z., Lin, Y., Cao, Y., Hu, H., Wei, Y., Zhang, Z., Lin, S., and Guo, B. Swin transformer: Hierarchical vision transformer using shifted windows. In *2021 IEEE/CVF International Conference on Computer Vision, ICCV 2021, Montreal, QC, Canada, October 10-17, 2021*, 9992–10002. IEEE, (2021).
- [56] Lewis, M., Liu, Y., Goyal, N., Ghazvininejad, M., Mohamed, A., Levy, O., Stoyanov, V., and Zettlemoyer, L. BART: denoising sequence-to-sequence pre-training for natural language generation, translation, and comprehension. In *Proceedings of the 58th Annual Meeting of the Association for Computational Linguistics, ACL 2020, Online, July 5-10, 2020*, 7871–7880, (2020).